Novel INK4 Proteins, p19 and p18, Are Specific Inhibitors of the Cyclin D-Dependent Kinases CDK4 and CDK6

HIROSHI HIRAI,[1] MARTINE F. ROUSSEL,[1] JUN-YA KATO,[1] RICHARD A. ASHMUN,[1,2]
AND CHARLES J. SHERR[1,3]*

Departments of Tumor Cell Biology[1] *and Experimental Oncology*[2] *and Howard Hughes Medical Institute,*[3]
St. Jude Children's Research Hospital, Memphis, Tennessee 38105

Cyclin D-dependent kinases act as mitogen-responsive, rate-limiting controllers of G_1 phase progression in mammalian cells. Two novel members of the mouse *INK4* gene family, p19 and p18, that specifically inhibit the kinase activities of CDK4 and CDK6, but do not affect those of cyclin E-CDK2, cyclin A-CDK2, or cyclin B-CDC2, were isolated. Like the previously described human INK4 polypeptides, p16[INK4a/MTS1] and p15[INK4b/MTS2], mouse p19 and p18 are primarily composed of tandemly repeated ankyrin motifs, each ca. 32 amino acids in length. p19 and p18 bind directly to CDK4 and CDK6, whether untethered or in complexes with D cyclins, and can inhibit the activity of cyclin D-bound cyclin-dependent kinases (CDKs). Although neither protein interacts with D cyclins or displaces them from preassembled cyclin D-CDK complexes in vitro, both form complexes with CDKs at the expense of cyclins in vivo, suggesting that they may also interfere with cyclin-CDK assembly. In proliferating macrophages, p19 mRNA and protein are periodically expressed with a nadir in G_1 phase and maximal synthesis during S phase, consistent with the possibility that INK4 proteins limit the activities of CDKs once cells exit G_1 phase. However, introduction of a vector encoding p19 into mouse NIH 3T3 cells leads to constitutive p19 synthesis, inhibits cyclin D1-CDK4 activity in vivo, and induces G_1 phase arrest.

Holoenzymes formed between D-type G_1 cyclins and their major catalytic partners, the cyclin-dependent kinases (CDKs) CDK4 and CDK6, facilitate progression through the first gap phase (G_1) of the mammalian cell division cycle (46). As cells enter the cycle from quiescence, the accumulation of these holoenzymes occurs in response to mitogenic stimulation, with their kinase activities being first detected in mid-G_1 phase and increasing as cells approach the G_1/S boundary (29, 32). The cyclin D regulatory subunits are highly labile, and premature withdrawal of growth factors in G_1 phase results in the rapid decay of cyclin D-CDK activity and correlates with the cell's failure to enter S phase. In contrast, removal of growth factors late in G_1 phase, although resulting in a similar collapse of cyclin D-CDK activity, has no effect on the cell's further progression through the cycle (30). Microinjection of antibodies to cyclin D1 into fibroblasts during G_1 prevents S phase entry, but injections performed at or after the G_1/S transition are without effect (2, 44). Therefore, cyclin D-CDK4 complexes execute critical functions at a restriction point late in G_1, after which cells become independent of mitogens for completion of the cycle.

Several observations argue for a role of the cyclin D-dependent kinases in phosphorylating the retinoblastoma protein, pRb. First, cyclin D-CDK complexes have a distinct substrate preference for pRb but do not phosphorylate the canonical CDK substrate, histone H1 (28, 29, 32). Their substrate specificity may be mediated in part by the ability of D-type cyclins to bind to pRb directly, an interaction which is facilitated by a Leu-X-Cys-X-Glu pentapeptide that the D cyclins share with DNA oncoproteins that also bind pRb (10, 15, 24). Second, cells in which pRb function has been disrupted by mutation or deletion or after transformation by DNA tumor viruses are no longer inhibited from entering S phase by microinjection of antibodies to D cyclin, indicating that they have lost their dependency on the cyclin D-regulated G_1 control point (26, 49). However, introduction of pRb into such cells restores their requirement for cyclin D function (26). Thirdly, pRb-negative tumor cells synthesize elevated levels of a 16-kDa polypeptide inhibitor of CDK4, p16[INK4a], which is found in complexes with CDK4 at the expense of D-type cyclins during G_1 phase (5, 45, 54). The fact that such cells cycle in the face of apparent CDK4 inhibition again implies that D-type cyclins are dispensable in this setting.

A 15-kDa CDK4 and CDK6-inhibitory protein, p15[INK4b], is induced in human epithelial cells treated by transforming growth factor β (TGF-β) (18), indicating that in contradistinction to the positive regulation of D-type cyclin synthesis by growth factors, extracellular inhibitors of G_1 progression can interfere with the activities of D-type CDKs by inducing INK4 proteins. During completion of this work, another human gene encoding an 18-kDa INK4 protein was isolated and mapped to human chromosome 1 (17). All INK4 proteins are composed of repeated 32-amino-acid ankyrin motifs, and unlike other universal CDK inhibitors, such as p21[Cip1/Waf1] (14, 16, 19, 52) and p27[Kip1] (42, 43, 50), they selectively inhibit the activities of CDK4 and CDK6 but not those of other CDKs (17, 18, 45). Here, we report the characterization of two mouse INK4 proteins, p19 and p18, the latter being the cognate of human p18. The novel INK4 family member, p19, is periodically expressed during the cell cycle, being maximally induced as cells enter S phase. When constitutively expressed, p19 inhibits cyclin D-dependent kinase activity in vivo and induces G_1 phase arrest.

MATERIALS AND METHODS

Yeast two-hybrid screen. A yeast two-hybrid screening system predicated on the technique of Fields and coworkers (3) as modified by Durfee et al. (13) was used to isolate cDNAs encoding proteins able to interact with CDK4. A *Bam*HI

---

fragment encoding the entire open reading frame of mouse CDK4 (28) was inserted into the *Bam*HI site of the plasmid pAS2, which contains the *TRP1* and *CYH* genes, conferring auxotrophy to tryptophan and sensitivity to cycloheximide, respectively (13). The resulting "bait" plasmid (pAS2cdk4) drives the expression from the alcohol dehydrogenase promoter of a GAL4-CDK4 fusion protein containing amino-terminal GAL4 DNA binding sequences (amino acids 1 to 147). Screening was performed with yeast strain Y190, which expresses two GAL4-inducible markers, *HIS3* and *LacZ*. Y190 cells containing pAS2cdk4 were transformed with *LEU2* pACT plasmids containing cDNAs (prepared from mouse T-lymphoma cells) which were fused 3′ to the GAL4 transcriptional activation domain (Clontech, Palo Alto, Calif.). Transformants were plated and selected for 9 days at 30°C on SD synthetic medium lacking leucine, tryptophan, and histidine and containing 50 mM 3-amino-1,2,4 triazole (3-AT). Of 1.6×10^7 transformants, 327 histidine-positive (HIS$^+$) colonies were obtained; these were lifted on Hybond-C nitrocellulose filters (Amersham, Arlington Heights, Ill.), frozen at −70°C for 15 min, thawed, and overlaid on Whatman 3M paper containing 60 mM Na$_2$HPO$_4$, 40 mM NaH$_2$PO$_4$, 10 mM KCl, 1 mM MgSO$_4$, 40 mM β-mercaptoethanol, and 0.033% X-Gal (5-bromo-4-chloro-3-indolyl-β-D-galactopyranoside). After a 20-h incubation at 30°C, 158 blue colonies were identified and streaked on synthetic medium lacking leucine and containing 2.5 or 10 μg of cycloheximide per ml in order to segregate pAS2cdk4, and the surviving colonies were restreaked on medium lacking either leucine or tryptophan to confirm plasmid segregation. Ninety-nine such colonies were mated with yeast strain Y187 containing either pAS2cdk4 or plasmids encoding other transactivating GAL4 fusion proteins (including the yeast kinase SNF1 and human lamin) by coincubation in yeast-peptone-dextrose (YPD) medium for 15 h at 30°C, and the progeny were streaked on SD synthetic medium lacking leucine, tryptophan, and histidine and containing 50 mM 3-AT. Eighty-three library plasmids which activated HIS3 and LacZ only in the presence of GAL4-CDK4 were isolated from yeast, used to transform *Escherichia coli* (strain HB101), grown up, and repurified.

Positive plasmids were dot blotted onto Hybond N filters and hybridized for 20 h at 42°C with a ^{32}P-labeled cyclin D probe (a 1:1:1 mixture of mouse cyclins D1, D2, and D3) in 3× SSC (1× SSC is 0.15 M NaCl plus 0.015 M sodium citrate) containing 35% formamide. Filters were washed in 1× SSC containing 0.1% sodium dodecyl sulfate (SDS) for 30 min at 65°C, yielding 29 positive clones. Several of the 54 remaining plasmid DNAs chosen at random were radiolabeled by nick translation and rehybridized to the filters, ultimately describing several families of related sequences. The nucleotide sequences of cDNA inserts from representative plasmids of each group were determined with a Sequenase version 2.0 kit (U.S. Biochemicals, Cleveland, Ohio). Thirty-six plasmids contained the coding sequences of two novel *INK4*-related genes, here designated p19 and p18 (see Results); the remaining eighteen plasmids contained nine sets of less abundant gene sequences, none of which showed significant homology to known sequences in GenBank.

Production of GST fusion proteins. Fragments containing the entire coding sequences for p19 and p18 were amplified by PCR with the following oligonucleotide primers: 5′p19, CCGGATCC*ATG*CTTCTGGAAGAAGT; 3′p19, CCG AATTCTCACATTGGGATCATCA; 5′p18, CCGGATCC*ATG*GCCGAGCC TTGGGG; 3′p18, CCGAATTCTCACTGCAGGCTTGTGG. The underlined ATGs in the sense strand oligonucleotides correspond to the p19 and p18 initiator codons, which were preceded by *Bam*HI sites to enable subsequent cloning. Products digested with *Bam*HI and *Eco*RI were inserted into pGEX-3X (Pharmacia, Uppsala, Sweden) in frame with glutathione *S*-transferase (GST). pGST-MAD3, a plasmid encoding mouse IκB, and pGST-ANK6, which encodes the MAD3 subdomain containing only the five ankyrin repeats (amino acids 73 to 242), were kindly provided by Lawrence Kerr (Vanderbilt University, Nashville, Tenn.).

Overnight cultures of bacteria transformed with plasmids encoding the GST fusion proteins were diluted 10-fold with fresh medium and cultured for 2 to 4 h at 37°C. Recombinant proteins were induced with 1 mM IPTG (isopropyl-β-D-thiogalactopyranoside) for 1 h at 37°C, and the harvested cells were lysed by sonication in phosphate-buffered saline containing 1% Triton X-100 and clarified by centrifugation. GST fusion proteins were adsorbed to glutathione-Sepharose beads (Pharmacia), washed with 50 mM Tris HCl (pH 7.5), and eluted in the same buffer containing 5 mM reduced glutathione (Sigma, St. Louis, Mo.). Proteins were dialyzed against 50 mM HEPES (*N*-2-hydroxyethylpiperazine-*N*′-2-ethanesulfonic acid; pH 7.5), 150 mM NaCl, and 1 mM EDTA and quantitated with a bicinchoninic acid assay kit (Pierce, Rockford, Ill.) with bovine serum albumin (BSA) as a protein standard.

In vitro protein binding assay. pBluescript plasmids containing the entire coding sequences of mouse CDK2, CDK4, CDK5, and CDK6 (27, 28) and of human CDC2/CDK1 and CDK3 (provided by Matthew Meyerson and Edward Harlow, MGH Cancer Center, Cambridge, Mass.) were transcribed and translated in vitro (27). Mouse CDK6 cDNA was cloned from a mouse macrophage library (Stratagene, La Jolla, Calif.) by screening with a full-length human CDK6 clone (also provided by M. Meyerson and E. Harlow). Following transcription and translation, rabbit reticulocyte lysates containing [^{35}S]methionine-labeled CDKs (20 to 40 μl) were diluted to 0.5 ml in IP kinase buffer (50 mM HEPES, pH 7.5, containing 150 mM NaCl, 1 mM EDTA, 1 mM dithiothreitol [DTT], and 0.1% Tween 20) containing 10 mg of BSA per ml and mixed with 1 μg of purified GST or GST-p19 immobilized on glutathione-Sepharose beads. After 2 h of

incubation at 4°C, the beads were collected by centrifugation and washed four times in IP kinase buffer, and the bound proteins were denatured and analyzed by electrophoresis on 12.5% polyacrylamide gels containing SDS (1).

Kinase inhibition assay. *Spodoptera frugiperda* (Sf9) cell lysates (2.5 to 5 μl, corresponding to 5×10^4 cells) containing CDKs and cyclins (24) were mixed with purified, soluble GST or the indicated GST fusion proteins in 10 μl of 50 mM HEPES buffer, pH 7.5, containing 10 mM MgCl$_2$ and 1 mM DTT, and incubated for 2 h at 4°C. Kinase activity was assayed in a 25-μl reaction mixture at 30°C for 20 min in the same buffer, to which 2.5 mM EGTA [ethylene glycol-bis(β-aminoethyl ether)-*N,N,N′,N′*-tetraacetic acid], 10 mM β-glycerophosphate, 0.1 mM sodium orthovanadate, 5 mM NaF, 20 μM ATP, and 5 μCi of [γ-^{32}P]ATP (6,000 Ci/mmol; Amersham) were added. Either 0.2 μg of soluble GST-pRb containing all pRb sequences required for inhibition of cell growth (15, 24) or 1 μg of histone H1 (Boehringer Mannheim) was used as a substrate. The reaction products were electrophoretically separated on denaturing gels, and phosphorylated proteins were detected by autoradiography.

For preparation of radiolabeled Sf9 lysates, cells infected with recombinant baculovirus vectors encoding cyclin D2 and CDK4 were metabolically labeled 40 h after infection for 8 h with 200 μCi of [^{35}S]methionine (specific activity, 1,000 Ci/mmol; ICN, Irvine, Calif.) per ml and harvested as described elsewhere (24). Portions of the lysate (7.5 μl) were diluted with 0.5 ml of IP kinase buffer containing 10 mg of BSA per ml, and GST-p19 (0.3 μg) was added as indicated prior to incubation for 2 h at 4°C. Complexes containing cyclin D2 and CDK4 were precipitated with rabbit antiserum to intact recombinant cyclin D2 (serum R$_T$) or to the C terminus of CDK4 (serum R$_Z$) preadsorbed to protein A-Sepharose beads (29). For detection of kinase activity in the immune complexes, the beads were washed twice in IP buffer and twice in kinase buffer without protease inhibitors, suspended in 25 μl of kinase reaction mixture, and assayed as described above. Phosphorylated GST-pRb and metabolically labeled cyclin D2 and CDK4 were resolved by electrophoresis on 12.5% polyacrylamide gels and detected by autoradiography.

Cell cycle analysis. Murine BAC1.2F5 macrophages were cultured in Dulbecco's modified Eagle's medium supplemented with 15% fetal bovine serum, 2 mM glutamine, 100 U of penicillin per ml, 100 μg of streptomycin per ml, and 25% L-cell-conditioned medium as a source of colony-stimulating factor 1 (CSF-1) (48). The cells were arrested in early G$_1$ phase by CSF-1 starvation for 18 h, after which they were restimulated with CSF-1 to reenter the cycle synchronously (30, 51). Cells (2×10^7 per datum point) were harvested at intervals thereafter, and the DNA content of representative aliquots was measured by flow-cytometric analysis of propidium iodide-stained nuclei (30). For preparation of RNA, washed cells were scraped into 4.2 M guanidine thiocyanate–0.1 M Na acetate (pH 5)–5 mM EDTA and layered over 2 M CsCl$_2$–0.1 M Na acetate–5 mM EDTA in a Beckman SW41 centrifuge tube. Following centrifugation at 33,000 rpm overnight, the pelleted RNA was suspended in 10 mM Tris HCl (pH 7.5), 10 mM EDTA, and 0.5% SDS, extracted twice with phenol and twice with chloroform, and precipitated with 2.5 volumes of ethanol at −20°C. RNA was separated electrophoretically in 1% agarose, blotted to nitrocellulose, and hybridized with the indicated cDNA probes at 42°C for 20 h in 5× SSPE buffer (1× SSPE is 0.15 M NaCl, 10 mM NaH$_2$PO$_4$, and 1 mM EDTA [pH 7.7]) containing 50% formamide (9). Filters were washed with 2× SSC containing 0.1% SDS first at 42°C and then at 65°C.

A synthetic peptide corresponding to the eight C-terminal amino acids of mouse p19 was conjugated to keyhole limpet hemocyanin and used to immunize rabbits (12). The antiserum precipitated radiolabeled mouse p19 produced by translation in vitro but did not cross-react with mouse p18 or human p16 produced in parallel. Asynchronously proliferating macrophages or synchronized cells prepared as described above (1×10^6 cells per time point) were metabolically labeled for 1 h with 200 μCi of [^{35}S]methionine per ml, and p19 immunoprecipitated from the cell lysates was resolved on denaturing polyacrylamide gels and detected by autoradiography by previously described methods (30). In some experiments, immunoprecipitated p19 resolved on gels was transferred to nitrocellulose and immunoblotted with antiserum to CDK4; sites of antibody binding were detected with ^{125}I-labeled *Staphylococcus aureus* protein A (11).

Enforced expression of p19 in mammalian fibroblasts. The *Bam*HI-*Eco*RI fragment encoding p19 and a *Hin*dIII-*Bam*HI fragment containing the entire coding sequence of mouse CD8 (55) were both subcloned into the pSRα-MSV-TK retrovirus vector (34), provided by Charles Sawyers, UCLA Medical Center, Los Angeles, Calif. In this construct, p19 is expressed under the control of viral long terminal repeat sequences, whereas CD8 expression is controlled by an internal thymidine kinase promoter. The plasmid was transfected into NIH 3T3 cells (8), and 48 h later, transfected cells were immunostained with anti-CD8, counterstained with propidium iodide, and analyzed by flow cytometry to determine the DNA content of gated CD8-positive and CD8-negative cells (25).

For virus production and infection, the same plasmid was cotransfected into 293T cells (40) (provided by David Baltimore) together with a plasmid encoding an ecotropic helper virus containing a defective virion-packaging (ψ2) sequence (34). Culture supernatants containing retroviruses harvested 48 to 72 h after transfection were used to infect proliferating NIH 3T3 fibroblasts. Infected cells were analyzed 48 h later by flow cytometry as described above or were lysed in IP kinase buffer, and cyclin D-CDK4 complexes were immunoprecipitated and assayed for Rb kinase activity (29).
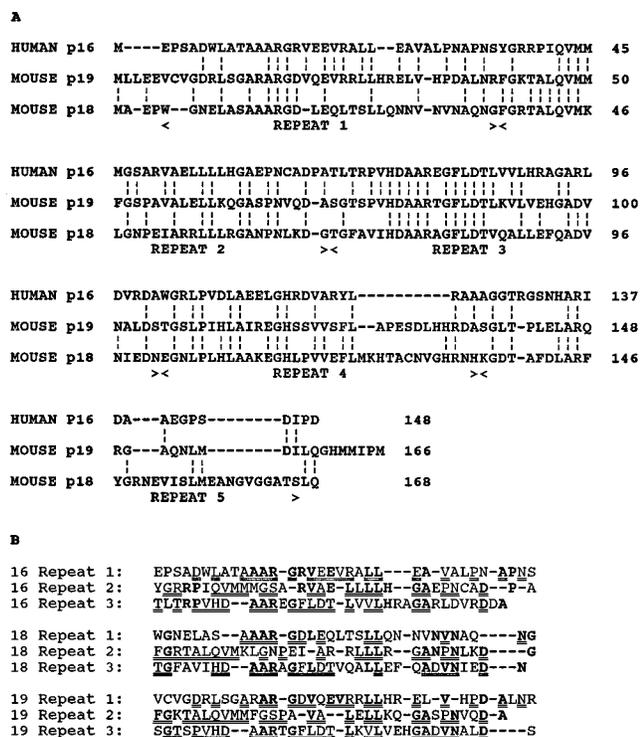
A

```
HUMAN p16   M----EPSADWLATAAARGRVEEVRALL--EAVALPNAPNSYGRRPIQVMM   45
                |  | |||| ||||| ||| |||| ||  |||   |      |||||
MOUSE p19   MLLEEVCVGDRLSGARARGDVQEVRRLLHRELV-HPDALNRFGKTALQVMM   50
             |  |   ||| | ||||| ||  | |||| |    ||    |  | ||||||
MOUSE p18   MA-EPW--GNELASAAARGD-LEQLTSLLQNNV-NVNAQNGFGRTALQVMK   46
                   <           REPEAT 1              ><

HUMAN p16   MGSARVAELLLLHGAEPNCADPATLTRPVHDAAREGFLDTLVVLHRAGARL   96
             ||  ||  ||||  | ||    |||   |||||| |||||| | |  |  ||
MOUSE p19   FGSPAVALELLKQGASPNVQD-ASGTSPVHDAARTGFLDTLKVLVEHGADV  100
             | |   |    ||| ||  |     |    |||||| ||||||| | ||| |
MOUSE p18   LGNPEIARRLLLLRGANPNLKD-GTGFAVIHDAARAGFLDTVQALLEFQADV   96
               REPEAT 2        ><            REPEAT 3

HUMAN p16   DVRDAWGRLPVDLAEELGHRDVARYL----------RAAAGGTRGSNHARI  137
             | | |   |  ||   ||||| |  |             |  | |   ||
MOUSE p19   NALDSTGSLPIHLAIREGHSSVVSFL--APESDLHHRDASGLT-PLELARQ  148
             |  |  |  |  |     |||  |  |        ||  | | |     ||
MOUSE p18   NIEDNEGNLPLHLAAKEGHLPVVEFLMKHTACNVGHRNHKGDT-AFDLARF  146
               ><             REPEAT 4               ><

HUMAN P16   DA---AEGPS--------DIPD       148
             |              ||||
MOUSE p19   RG---AQNLM--------DILQGHMMIPM  166
             |      ||         ||
MOUSE p18   YGRNEVISLMEANGVGGATSLQ       168
               REPEAT 5        >
```

B

```
16 Repeat 1:  EPSADWLATAAAR-GRVEEVRALL---EA-VALPN-APNS
16 Repeat 2:  YGRRPIQVMMGSA-RVAE-LLLLH--GAEPNCAD--P-A
16 Repeat 3:  TLTRPVHD--AAREGFLDT-LVVLHRAGARLDVRDDA

18 Repeat 1:  WGNELAS--AAAR-GDLEQLTSLLQN-NVNVNAQ----NG
18 Repeat 2:  FGRTALQVMKLGNPEI-AR-RLLLR--GANPNLKD----G
18 Repeat 3:  TGFAVIHD--AARAGFLDTVQALLEF-QADVNIED---N

19 Repeat 1:  VCVGDRLSGARAR-GDVQEVRRLLHR-EL-V-HPD-ALNR
19 Repeat 2:  FGKTALQVMMFGSPA-VA--LELLKQ-GASPNVQD-A
19 Repeat 3:  SGTSPVHD--AARTGFLDT-LKVLVEHGADVNALD----S
```

FIG. 1. Amino acid sequences of mouse p19 and p18. (A) The predicted amino acid sequences of mouse p18 and human p16[INK4a] were aligned with that of mouse p19, with the Intelligenetics FAST DB computer program. The limits of the ankyrin repeats are indicated by the arrows below the line. (B) Ankyrin repeats 1 to 3 of human p16 and of mouse p18 and p19 were aligned with each other by eye. Sequences shared between at least two of three repeats within the same protein (e.g., between repeats 1 and 2 of p16) are indicated by boldface type, whereas sequences shared by cognate repeats in at least one of the two homologous proteins (e.g., by repeats 1 in p19 and p18) are demarcated by double underlines.

RESULTS

Isolation of mouse p19 and p18. A yeast two-hybrid screen was used to isolate cDNAs from a mouse T-cell lymphoma library encoding proteins able to interact with CDK4. From 1.6×10^7 colonies, 29 isolated cDNAs encoded D-type cyclins and 36 others encoded two novel products of members of the *INK4* gene family, which are here designated p19 (represented by 29 clones) and p18 (7 additional clones). The nucleotide sequences of these two mouse *INK4* family members predict polypeptides of 166 (p19) and 168 (p18) amino acids with molecular masses of 18,005 and 18,176 Da, respectively. When the two cDNAs were transcribed and translated in vitro and electrophoretically separated in parallel on a denaturing 15% polyacrylamide gel, p19 migrated more slowly than p18, prompting us to designate the proteins on the basis of their apparent molecular masses. The two proteins are approximately 40% identical to one another and have similar degrees of amino acid homology with the previously described human p16[INK4a] and p15[INK4b] polypeptides. Like the latter, p19 and p18 are composed of tandem ankyrin motifs, each about 32 amino acids in length (Fig. 1A). The most highly conserved regions of mouse p19 and p18 include the amino acid sequences constituting repeats 1 to 3 and half of repeat 4. p18 has

a fifth repeat, whereas the corresponding sequences in mouse p19 and human p16 are much less well conserved (Fig. 1A). Repeats 1 to 3 of p16, p18, and p19 could be aligned with one another as well as with those of other family members (Fig. 1B).

After completion of this work, the sequence of human p18 was reported (17). The human and mouse p18 polypeptides, each 168 amino acids in length, are identical over 153 residues, with seven of the substitutions occurring in the least conserved C-terminal domain (residues 140 to 168). To avoid redundancy, the following presentation emphasizes the properties of p19.

Mouse INK4 proteins specifically inhibit CDK4 and CDK6 kinases. Human INK4 polypeptides specifically bind to the cyclin D-dependent catalytic subunits CDK4 and CDK6 (5, 18, 45). To study the interactions of mouse p19 and p18 with CDKs, cDNAs encoding CDC2 (CDK1) and CDKs 2 to 6 were transcribed and translated in vitro, and the radiolabeled products were mixed with GST-tagged p19 and p18 fusion proteins adsorbed to glutathione-Sepharose beads or to GST-Sepharose beads as a control. As reported previously (27), several CDK translation products were produced from each template, with major radiolabeled species in the 34-kDa range being obtained with the CDC2, CDK2, CDK4, and CDK5 cDNAs (Fig. 2A, lanes 1, 2, 4, and 5). The predominant CDK6 species was ca. 38 kDa (Fig. 2A, lane 6), as predicted from its nucleotide sequence (4, 31), but CDK3 products were significantly larger than expected, because of improper translational termination (lane 3) (27). None of the radiolabeled translation products bound to control glutathione-Sepharose beads (Fig. 2A, lanes 7 to 12), and only the CDK4 and CDK6 proteins efficiently bound to beads containing the GST-p19 fusion protein (lanes 16 and 18). In the same assay, D-type cyclins were unable to interact with GST-p19 beads (Fig. 2B). Virtually identical results were obtained with GST-p18 (data not shown, but see below).

To determine whether their binding could inhibit CDK4 and CDK6 activity, bacterially produced p19 and p18 fusion proteins were mixed at different concentrations with extracts containing enzymatically active complexes of cyclin D2-CDK4 and cyclin D2-CDK6 produced in baculovirus vector-infected insect cells, and the enzymes were assayed for pRb kinase activity (24). Figure 3 shows that addition of the GST-p19 fusion protein reduced the pRb kinase activity of the cyclin D2-CDK4 (panel A) and cyclin D2-CDK6 (panel B) holoenzymes (lanes 2 to 7) to background levels equal to those observed with extracts of cells infected with a control, wild-type baculovirus (lanes 1). GST-p19 was as potent as human p16 in inhibiting the pRb kinase activity of either cyclin D-CDK4 or cyclin D-CDK6 (Fig. 3A and B, lanes 9 to 11). However, addition of up to 1 µg of a control GST protein had no effect on either enzyme (Fig. 3, lanes 8).

Although human p18 was reported to have greater affinity for CDK6 than for CDK4 (17), the murine GST-p18 fusion protein was as potent as GST-p19 in inhibiting both kinases in vitro (Fig. 3C and D, lanes 2 to 7). However, not all proteins containing repeated ankyrin motifs can effectively inhibit these enzymes. Mouse IκB (MAD3), for example (Fig. 3C and D, lanes 9 and 10), or a subdomain of the protein containing only the ankyrin repeats (lanes 11, 12) was at least 30-fold less efficient in extinguishing CDK4 and CDK6 activities than were the p19 and p18 fusion proteins. Moreover, although combinations of CDK4 with any of the D-type cyclins proved to be effective substrates for p19-mediated inhibition (Fig. 4A, lanes 1 to 10), p19 neither attenuated the pRb kinase activity of cyclin E-CDK2 (Fig. 4A, lanes 11 to 13) nor affected the
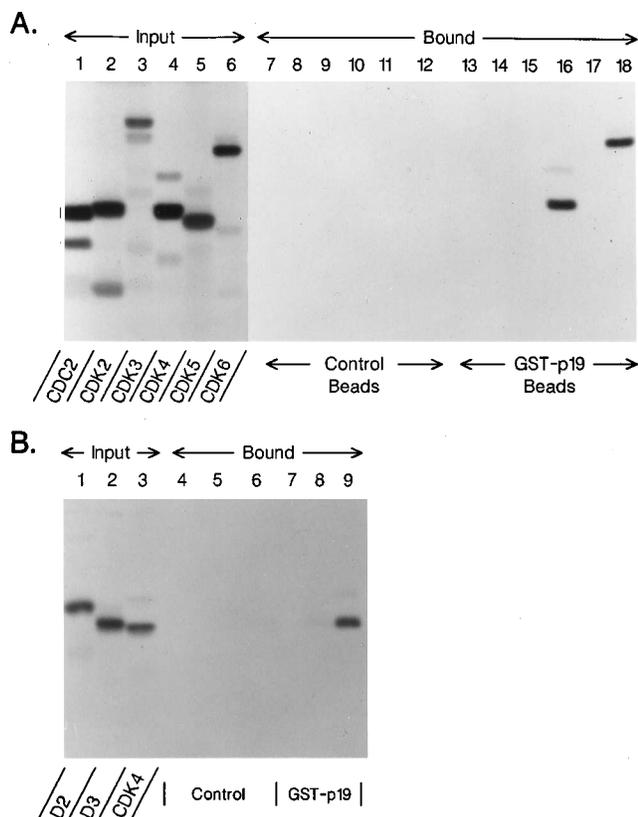
A.

B.

FIG. 2. Binding of mouse p19 to CDK4 and CDK6. (A) Plasmids containing cDNA coding sequences of the CDKs indicated in the legend below lanes 1 to 6 were transcribed and translated in vitro, and aliquots of the [³⁵S]methionine-labeled products were separated by electrophoresis on denaturing polyacrylamide gels. Equal aliquots of the inputs shown in lanes 1 to 6 were incubated with control GST-Sepharose beads (lanes 7 to 12) or with beads containing a GST-p19 fusion protein (lanes 13 to 18). The beads were washed, and adsorbed radiolabeled products were separated on gels. (B) The experiment shown in panel A was repeated, except that radiolabeled cyclins D2 and D3 were substituted for CDKs; CDK4 was used as the positive control. All autoradiographic exposure times were 15 h.

histone H1 kinase activity of cyclin E-CDK2, cyclin A-CDK2, or cyclin B-CDC2 (Fig. 4B). Again, similar data were obtained with mouse p18 (data not shown). Therefore, both p19 and p18 interact specifically with CDK4 and CDK6 to inhibit their pRb kinase activities in complexes with D-type cyclins.

Mouse p19 does not displace cyclin D from preassembled complexes with CDK4. In cells that fail to express a functional pRb protein, p16^INK4a is found in a complex with CDK4 at the expense of cyclin D (5, 45). Therefore, p16^INK4a might compete with cyclin D for binding sites on CDK4, extinguishing its activity by displacing the positive regulator. When metabolically labeled lysates from baculovirus-infected Sf9 cells containing cyclin D2 and CDK4 were immunoprecipitated with antibodies to the individual subunits, antibodies to either subunit coprecipitated the other (Fig. 5A, lanes 2 and 3; the relevant [³⁵S]methionine-labeled bands are indicated at the right margin). In the experiment shown, lysates from coinfected Sf9 cells contained much more cyclin D2 than CDK4. Therefore, the antiserum to CDK4 coprecipitated equal amounts of CDK4 and cyclin D in a 1:1 molar complex (Fig. 5A, lane 3), while that directed to cyclin D also precipitated excess unbound cyclin subunits (lane 2). Under these conditions, all CDK4 was bound to cyclin, and in agreement, the
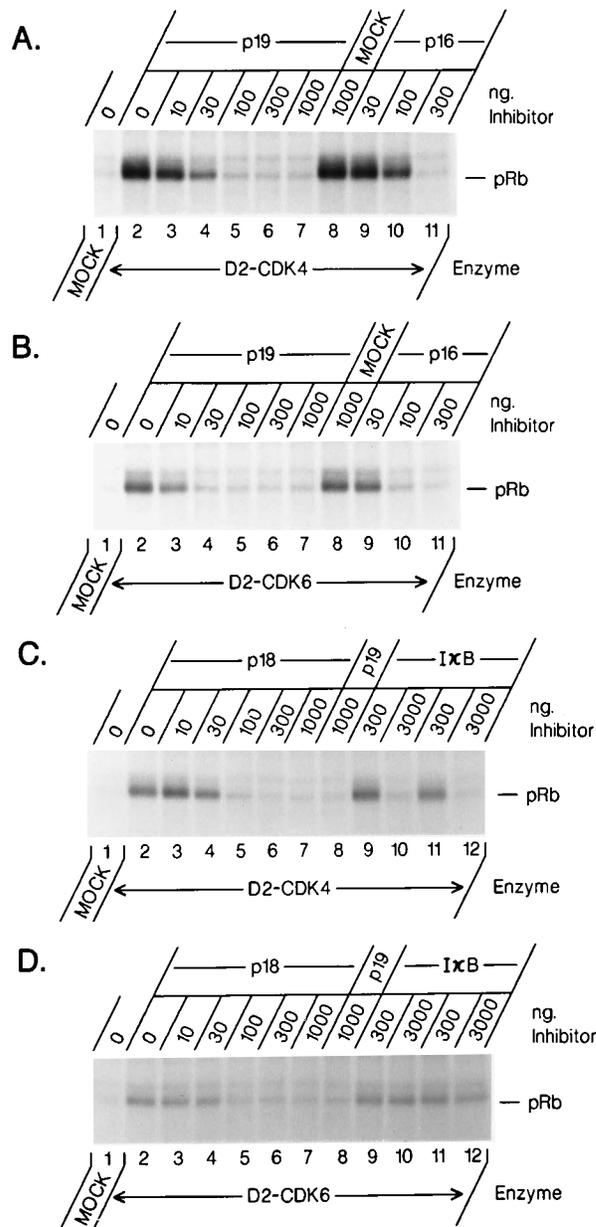
A.

B.

C.

D.

FIG. 3. p19 and p18 inhibit the pRb kinase activities of cyclin D-CDK4 and cyclin D-CDK6. Active holoenzyme complexes composed of cyclin D2-CDK4 (A and C) and cyclin D2-CDK6 (B and D) were produced in insect Sf9 cells coinfected with the appropriate vectors (24). Sf9 extracts infected with a wild-type baculovirus were used as controls for background kinase activity. GST fusion proteins containing the complete coding sequences of mouse p19 and p18 or human p16 were purified and eluted from glutathione-Sepharose beads, and the amounts of protein (in nanograms) indicated above each lane were added to fixed quantities of Sf9 lysates containing the indicated enzymes. The extracts were then assayed for pRb kinase activity as described elsewhere (24), and the products were resolved on denaturing gels. Panels C and D show similar experiments with GST proteins containing either mouse IκB (MAD3) (lanes 9 and 10) or a subdomain of the protein (amino acids 73 to 242) containing its ankyrin repeats (lanes 11 and 12). The autoradiographic exposure times were 15 h.

washed immune complexes recovered after precipitation with either antiserum contained similar amounts of pRb kinase activity (Fig. 5A, lanes 2 and 3; phosphorylated pRb is indicated at the right margin). When p19 was added to these lysates prior to immunoprecipitation, pRb kinase activity in
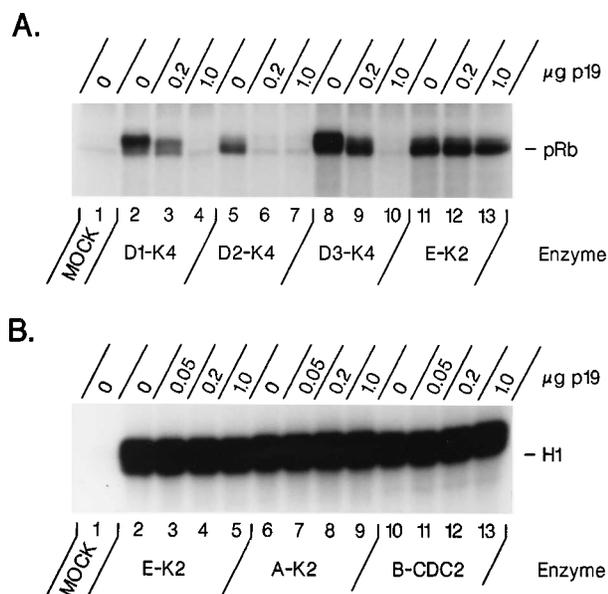
FIG. 4. p19 specifically inhibits cyclin D-dependent kinases. Insect extracts containing the holoenzymes indicated below each panel or those derived from cells infected with a wild-type baculovirus (mock, lanes 1) were incubated with the amounts of purified GST-p19 protein indicated at the tops of both panels. The extracts were then assayed for pRb kinase activity (A) or for histone H1 kinase activity (B), and the products of the reactions were resolved on denaturing gels. Exposure times were 15 h for panel A and 4 h for panel B.
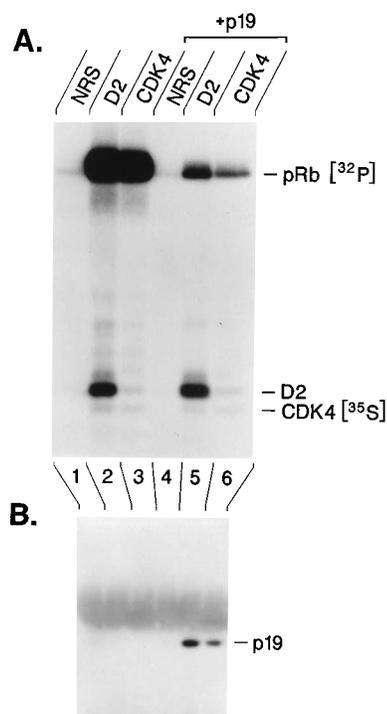

FIG. 5. Binding of p19 to the cyclin D2-CDK4 complex and inhibition of pRb kinase activity. Insect cells coinfected with baculovirus vectors encoding both CDK4 and cyclin D2 were metabolically labeled for the final 8 h of infection with [^{35}S]methionine. Lysates containing radiolabeled CDK4 and cyclin D2 were distributed into six equal aliquots, and purified p19 protein (0.3 μg) was added to three of the indicated samples (lanes 4 to 6). Samples were divided in half and precipitated with nonimmune rabbit serum (NRS) or with the indicated antiserum to cyclin D2 or CDK4. (A) Washed immune complexes obtained from one set of precipitates were assayed for pRb kinase activity, after which the reaction products were separated on denaturing gels. The positions of ^{32}P-labeled pRb and [^{35}S]methionine-labeled cyclin D2 and CDK4 are indicated in the right margin. The autoradiographic exposure time was 15 h. (B) The duplicate set of precipitates was separated on gels, transferred to nitrocellulose, and blotted with antiserum to p19.

recovered immune complexes was greatly inhibited (Fig. 5A, lanes 5 and 6), but the amount of cyclin D in the complexes was not significantly reduced (lane 6 compared with lane 3). Under these conditions, similar amounts of p19 were recovered in immune complexes generated with antiserum to cyclin D2 or CDK4 (Fig. 5B, lanes 5 and 6), even though cyclin D does not interact with p19 directly (see above). p19 was not trapped in complexes prepared with nonimmune rabbit serum (Fig. 5B, lane 4). Therefore, p19 can bind to the cyclin D-CDK4 holoenzyme and directly inhibit its activity without disrupting the interaction between cyclin D and CDK4. In separate experiments, we confirmed that cyclin D2-CDK4 complexes also bind human p16^{INK4a} with a concomitant loss in enzyme activity but no displacement of the cyclin (data not shown).

Mouse p19 and p18 are expressed in many normal tissues. A single class of p19 mRNA transcripts 1.3 kb in length was detected in a variety of mouse cell lines, as well as in many mouse tissues (Fig. 6). The p19 cDNA was isolated from thymic lymphoma cells, and relatively high levels of this mRNA were detected in hematopoietic organs, such as bone marrow and spleen (Fig. 6B), as well as in blood cell lines including MEL (erythroid); 32D, DA-3, and FDC-P1 (immature myeloid); BAC1.2F5 (macrophages); and CTLL-2 (T cells) (Fig. 6A). As reported for its human cognate (17), the patterns of expression of p18 were more complex. First, at least three forms of mRNA were observed, and these were differentially expressed in various tissues. Note, for example, that skin and lung primarily express a p18 transcript of 1.1 kb, whereas the predominant mRNA in bone marrow and spleen is considerably larger (1.9 kb). Unlike the human *INK4a* and *INK4b* genes, which are deleted in a high percentage of established cell lines, both p19 and p18 expression can be readily detected.

Expression of p19 during the macrophage cell cycle. Because both p19 and p18 are expressed in bone marrow-derived macrophages, we were able to study their regulation throughout the cell cycle. BAC1.2F5 macrophages arrest in early G$_1$ phase when deprived of CSF-1 for 18 to 22 h and can be induced to reenter the cell cycle synchronously by readdition of the growth factor (30, 51). Figure 7 shows that p19 mRNA could be detected in starved, quiescent cells (time 0) but decreased in abundance as cells entered G$_1$ phase. However, as cells approached the G$_1$/S transition (ca. 10 h), p19 mRNA synthesis was abruptly reinitiated and increased as the cells progressed through the remainder of the cycle. Maximal cell division occurred at 18 to 20 h. Although the cells rapidly lost synchrony in the second cycle and the second G$_1$ phase was shorter than the first (30), p19 levels again fell during G$_1$ (ca. 22 to 28 h) but increased in S phase (32 to 36 h). The relative abundance of p19 mRNA, determined by scanning the Northern (RNA) blots with a PhosphoImager, is summarized graphically at the bottom of Fig. 7. Virtually identical results were obtained with NIH 3T3 cells induced to reenter the cell cycle from quiescence by serum readdition (data not shown).

During reentry into the cell cycle, p18 mRNA was induced with kinetics similar to that of p19. However, CSF-1-starved macrophages expressed the 1.1-kb p18 mRNA species, whereas only the 1.9-kb form was induced at the G$_1$/S transition and remained elevated until cells reentered another cycle.
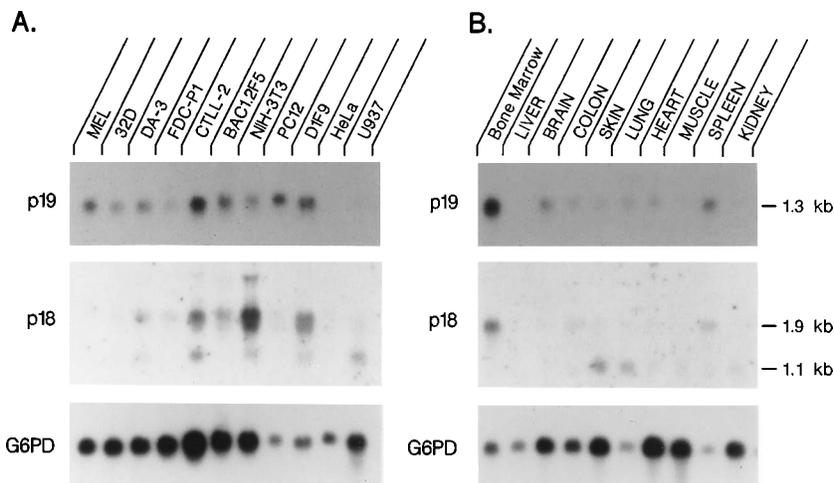
FIG. 6. Expression of p19 and p18 mRNAs in cell lines and mouse tissues. Total cellular RNA was extracted from the indicated cell lines (A) or mouse tissues (B), electrophoretically separated on agarose gels containing formamide (10 μg per lane), transferred to nitrocellulose, and hybridized with the indicated ^{32}P-labeled cDNA probes. Autoradiographic exposure times were 5 days (p19), 12 days (p18), and 2 days (G6PD).

The kinetics of induction of the p19 and p18 mRNAs in the first cycle were similar to that of cyclin A, which is also induced near the G_1/S boundary (41), but are readily distinguished from those of cyclin D1 mRNAs, which are induced early in G_1 phase and oscillate only modestly as cells continue to proliferate (30). The expression of a housekeeping gene, glucose 6-phosphate dehydrogenase (G6PD), showed minimal oscillation throughout the cycle, although its mRNA was somewhat less abundant in growth factor-deprived cells.

An antipeptide serum directed to the p19 C terminus could be used to immunoprecipitate the metabolically labeled protein from proliferating mouse cells (Fig. 8A, lanes 1 and 4). The immunoprecipitated 19-kDa protein was inhibited by competition with the cognate peptide (Fig. 8, lanes 2 and 5) but not with an unrelated peptide based on the CDK2 C terminus (lane 3). p19 immunoprecipitates also contained CDK4 (Fig. 8B, lane 2) but did not contain detectable levels of cyclin D1 (negative data not shown). Similar results were obtained with cell lines expressing CDK6. Thus, although p19 can bind to preassembled cyclin D-CDK4 complexes in vitro (Fig. 5), like other INK4 proteins, it may preferentially interact with unbound CDK4 and CDK6 in vivo. One possibility is that cyclin D-CDK complexes are inhibited from assembling during the latter phases of the cell cycle when INK4 proteins are actively synthesized. Consistent with the kinetics of p19 mRNA expression in synchronized macrophages (Fig. 7), synthesis of p19 protein was first detected near the G_1/S boundary, decreased as cells divided and reentered a second G_1 phase, and increased again during the following S phase (Fig. 8C). Hence, p19 mRNA and protein synthesis are periodic with relative nadirs during G_1 phase.

p19 can arrest G_1 progression. Expression of p19 is extinguished during G_1 phase as cyclin D-CDK4 (or CDK6) executes its critical functions. We therefore wished to determine whether constitutive expression of p19 would specifically arrest the cell cycle in G_1 phase. To this end, we inserted the p19 cDNA into a retroviral expression vector that also encodes the CD8 cell surface antigen. Asynchronously proliferating mouse NIH 3T3 fibroblasts were transfected with CD8 vectors lacking or containing p19 cDNA, and 48 h later the transfected cells were analyzed for both CD8 expression and DNA content by two-color flow cytometry. Cells transfected with the vector encoding both CD8 and p19 yielded a proportion of untransfected recipients that exhibited background CD8 fluorescence and were distributed throughout the cell cycle (delimited by box R1 in Fig. 9A and B). By contrast, 85% of those cells that expressed high levels of CD8 antigen (gated in box R2) exhibited a 2N DNA content characteristic of those in G1 phase (Fig. 9A and B). Cells transfected with the control CD8 expression vector, whether CD8 positive or not, were distributed throughout the cell cycle in a manner indistinguishable from those of untransfected cells (54.6% ± 4.9% were G_1, 36.5% ± 3.1% were S, and the remainder were G_2/M [means ± standard deviations]), indicating that transfection per se was not toxic and did not induce cell cycle arrest. In five independent experiments, transfection with the CD8 vector coexpressing p19 increased the proportion of cells in G_1 by 22% ± 12%, whereas transfection with the control CD8 vector had no effect. Analogous results were obtained with vectors encoding p18 (data not shown).

By cotransfection of the p19 vector plasmid together with a second plasmid providing retroviral helper functions into simian virus 40 T-antigen-positive 293T cells, virions that were capable of efficiently infecting NIH 3T3 cells were produced. Within 48 h of infection, the majority of such cells became CD8 positive and exhibited a concomitant (18% ± 3%) increase in their G_1 fraction compared with cells infected with the control CD8 vector lacking p19 cDNA. Cells harvested upon completion of the experiment, unlike proliferating NIH 3T3 cells, lacked detectable cyclin D-dependent kinase activity (Fig. 9C, lanes 9 to 11). Even with use of cells engineered to overexpress cyclin D (44), in which the levels of cyclin D-dependent kinase are elevated 5- to 10-fold (29), infection with the p19 vector almost completely inhibited cyclin D-dependent kinase (or CDK4 kinase) activity (Fig. 9C, lanes 1 to 8). Immunoblotting confirmed that these G_1-arrested populations ectopically expressed p19, which coprecipitated with CDK4 but not with cyclin D (data not shown), again suggesting that p19 may limit the formation of cyclin D-CDK4 complexes. Therefore, G_1-phase arrest induced by constitutive p19 expression is accompanied by inhibition of cyclin D-dependent kinase activity in vivo.
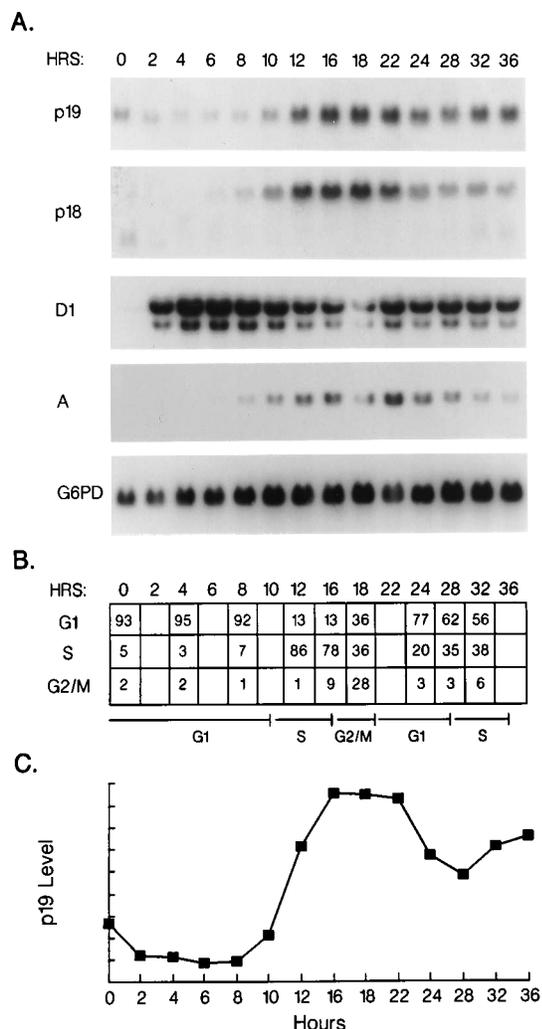
A.

B.

HRS:	0	2	4	6	8	10	12	16	18	22	24	28	32	36
G1	93		95		92		13	13	36		77	62	56	
S	5		3		7		86	78	36		20	35	38	
G2/M	2		2		1		1	9	28		3	3	6	

C.

FIG. 7. Expression of p19, p18, and different cyclins during the macrophage cell cycle. BAC1.2F5 macrophages arrested in early G₁ phase by CSF-1 starvation for 18 h were restimulated with CSF-1 to enter the cell cycle synchronously. (A) Total RNA extracted from cells at the indicated times (in hours) were subjected to Northern blotting analysis with the probes indicated at the left margin. (B) The different cell cycle phases were determined by flow-cytometric analysis of cellular DNA content. The cells lost synchrony as they progressed into the second cell cycle, and their second G₁ phase was shorter than the first (30). (C) Concentrations of p19 mRNA, as quantitated with a PhosphoImager. Exposure times for the Northern blots were 6 days for p19, 8 days for p18, 2 days for cyclins D1 and A, and 1 day for G6PD mRNA.

DISCUSSION

Both p19 and p18 share the cardinal structural and biochemical properties of previously described human *INK4* gene products, p16^INK4a and p15^INK4b. They are composed of repeated ankyrin motifs, bind to CDK4 and CDK6, and specifically inhibit the pRb kinase activities of cyclin D-CDK4 and cyclin D-CDK6 complexes. p19 (and, in our hands, human recombinant p16 as well) can bind to binary cyclin D-CDK4 complexes and inhibit their activity in vitro without displacing cyclin D. However, while antibodies to p19 coprecipitated CDK4 and CDK6 from lysates of proliferating mammalian cells, cyclin D was not detected in these complexes, suggesting that p19 might preferentially interact with the uncomplexed forms of these CDKs in vivo or might prevent their assembly with cyclin during those phases of the cell cycle when p19 is actively
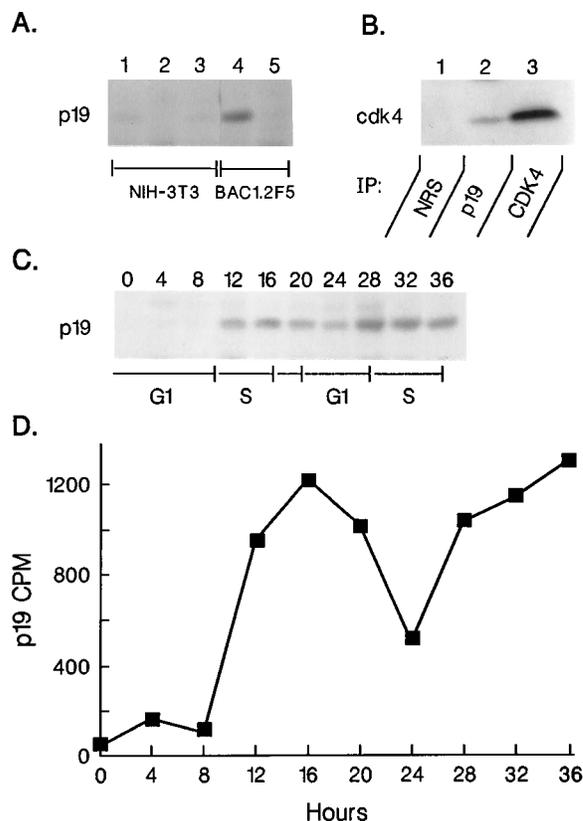
A.

B.

C.

D.

FIG. 8. p19 protein expression. (A) NIH 3T3 fibroblasts (lanes 1 to 3) and BAC1.2F5 macrophages (lanes 4 and 5) were metabolically labeled with [³⁵S]methionine for 1 h, and cell lysates immunoprecipitated with antiserum directed to a synthetic peptide based on the p19 C terminus were resolved on denaturing gels. No p19 was detected after competition with the cognate peptide (lanes 2 and 5), whereas an unrelated peptide was without effect (lane 3). (B) Lysates of BAC1.2F5 macrophages were immunoprecipitated with nonimmune rabbit serum (NRS, lane 1), antiserum to the p19 C terminus (lane 2), and antiserum to CDK4 (lane 3). Complexes separated on denaturing gels were transferred to nitrocellulose and immunoblotted with antiserum to CDK4. (C) CSF-1-starved macrophages stimulated to synchronously reenter the cycle (as shown in Fig. 7) were pulse labeled for 1 h at the indicated times (in hours) with [³⁵S]methionine, and precipitates prepared with antiserum to the p19 C terminus were separated on denaturing gels. (D) Rates of synthesis of p19 throughout the cell cycle, as determined by phosphorimaging analysis of the data shown in panel C. Exposure times were 5, 2, and 4 days for panels A, B, and C, respectively.

synthesized. Interactions with CDK4 and CDK6 appear quite specific to the INK4 subfamily of ankyrin repeat proteins in the sense that other proteins containing these motifs, such as IκB, bind only weakly to these CDKs and inhibit their activities in vitro only if added in quantities at least 30-fold in excess of those of the INK4 polypeptides. The fact that cDNAs encoding p19 were as frequently isolated as the type D cyclins from the yeast two-hybrid screen, whereas other ankyrin repeat proteins (apart from p18) were not identified among the remaining interacting clones, provides additional confidence in the specificity of its association with CDK4. In turn, the INK4 proteins as a group fail to inhibit other cyclin-CDK complexes, including cyclin E-CDK2, cyclin A-CDK2, and cyclin B-CDC2, and they do not bind to CDC2, CDK2, CDK3, or CDK5 in vitro. Therefore, these proteins are likely to play physiologic roles as specific regulators of CDK4 and CDK6 activity in vivo.

Mouse p19 and p18 exhibit only ca. 40% amino acid identity to one another, and both show similarly limited degrees of homology to human p16^INK4a and p15^INK4b. In contrast, mouse
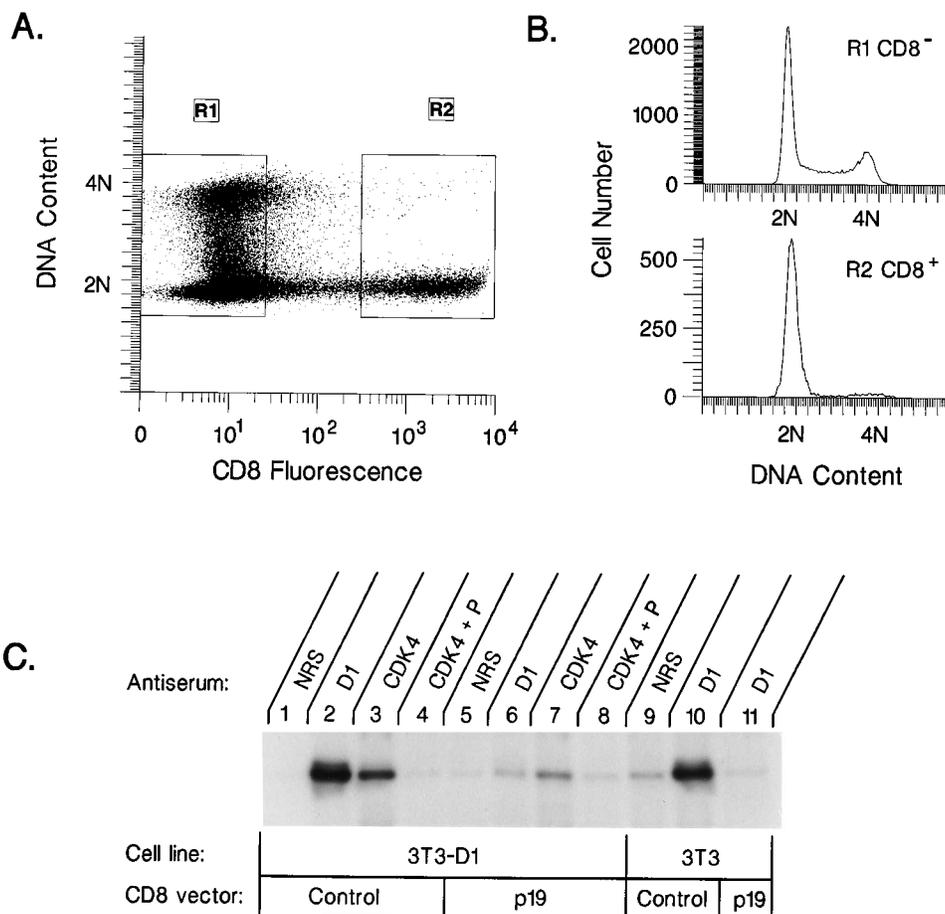
FIG. 9. Vector-mediated p19 expression induces G_1 phase arrest. NIH 3T3 cells transfected with a vector encoding both p19 and CD8 were analyzed 48 h later for CD8 fluorescence and DNA content (A). Cells yielding a fluorescence profile equivalent to those obtained with CD8-negative fibroblasts (box R1) and those expressing the highest level of CD8 antigen (box R2) were separately gated and analyzed for DNA content (B). (C) Immunoprecipitates from NIH 3T3 fibroblasts infected with a control CD8 vector or a vector containing p19 (as indicated at the bottom of the panel) were analyzed 48 h later for pRb kinase activity. Immune complexes were obtained with normal rabbit serum (NRS), monoclonal antibody (D1-72-13G) to cyclin D1 (D1), antiserum to the CDK4 C terminus (CDK4), or antiserum to CDK4 plus competing cognate peptide (CDK4+P), as indicated at the top of the panel. Precipitates were prepared from cells engineered to overexpress cyclin D1 (3T3-D1, lanes 1 to 8) or from parental NIH 3T3 cells (3T3, lanes 9 to 11). To obtain matched autoradiographic signals, lysates were prepared from 1/8 the number of 3T3-D1 cells as of parental cells. Exposure time, 8 h.

p19 and p18 exhibit >90% amino acid identity with their human counterparts. Human p16 and p15 map in tandem on the short arm of human chromosome 9 (22). The human homolog of mouse p19 maps to chromosome 19 (38), and p18 has been assigned to chromosome 1 (17), indicating that the *INK4* family includes a minimum of four distinct genes. We therefore suggest that the p18 and p19 genes be designated *INK4c* and *INK4d*, respectively.

Expression of p18[INK4c] and p19[INK4d] mRNAs can be readily detected in mouse tissues and cell lines, where they appear to oscillate throughout the cell cycle. Several forms of p18 mRNA which were differentially regulated in various tissues were observed, whereas the pattern of p19 expression was less complex, with only a single 1.3-kb mRNA observed. In synchronized macrophages, the abundance of p19 mRNA temporally correlated with the rates of p19 protein synthesis observed throughout the cell cycle, with the levels of mRNA and protein reaching a nadir in G_1 phase, abruptly increasing as cells entered S phase, and declining again as cells completed mitosis and reentered G_1. Introduction of a vector encoding p19 into NIH 3T3 fibroblasts led to G_1-phase arrest, indicating that p19 synthesis during the G_1 interval, but apparently not during

later phases, can halt cell cycle progression. Cyclin D1-dependent (CDK4) kinase activity was markedly reduced in cells engineered to ectopically express p19, including those that were engineered to overexpress cyclin D1, demonstrating that p19 has potent CDK4 inhibitory activity in vivo. The simplest interpretation is that p19-mediated inhibition of CDK4 kinase activity renders such cells unable to transit a cyclin D-dependent G_1 phase control point, but we cannot formally exclude the possibility that p19 might also mediate effects via other as yet unidentified targets. For example, p19 was independently cloned in a two-hybrid screen with the orphan steroid receptor Nur77 (NGFI-B) as bait, pointing to potential protein-protein interactions between p19 and transcription factors (7).

Because all INK4 proteins have similar biochemical properties, it remains unclear how each would contribute to CDK4 and CDK6 regulation in vivo. Although in vitro assays for CDK inhibition did not define significant differences in the abilities of p19, p18, and p16 to interfere with the activities of different binary cyclin D-CDK complexes assembled in insect cells, their specificities in vivo might depend upon their binding to higher-order holoenzyme complexes (53, 56) or on their ability to make independent contacts with CDK-associated proteins

other than D cyclins. The INK4 proteins might also be regulated in a cell lineage-specific manner, with individual ones responding differentially to antiproliferative signals. For example, p15 is specifically induced in human keratinocytes by TGF-β (18). By analogy, induction of p19 during G$_1$ phase would be expected to provoke cell cycle arrest. However, its ubiquitous expression in cell lines and tissues and its periodic expression during the cell cycle also connote a function in proliferating cells.

Further complexity stems from observations that greatly elevated levels of p16 synthesis have been detected in tumor cells lacking a functional pRb protein (5, 45, 54). Why should a CDK inhibitor be induced in cells that exhibit an apparent proliferative advantage over their normal counterparts? One explanation may be that p16 expression is governed by pRb-tethered transcription factors whose release from pRb constraint is triggered by CDK-mediated pRb phosphorylation late in G$_1$ phase. Induction of p16 in S phase might then act to extinguish CDK4 kinase activity after pRb undergoes phosphorylation, but in pRb-negative cells the protein would be expressed throughout the cell cycle (45). Consistent with this hypothesis, cyclin D1-dependent (CDK4/CDK6) kinase activities appear to be no longer required for G$_1$-phase progression in cells lacking functional pRb, but reintroduction of pRb reconfers sensitivity to cyclin D1-mediated control (26). Thus, pRb appears to be a critical if not exclusive target of CDK4 and *INK4a* undergoes frequent homozygous deletions and mutations in established cell lines (22, 35, 37, 39) and primary tumors (6, 20, 21, 23, 33, 36, 47), implying that, like pRb, it functions as a tumor suppressor. In certain tumor types, there is an inverse correlation between disruption of pRb function and deletion of p16, with cells either being pRb$^+$/p16$^-$ or pRb$^-$/p16$^+$ (37, 39). These findings underscore a dependency between p16- and pRb-mediated growth suppression and again argue that the two proteins function in a common biochemical pathway. While oscillatory synthesis of p16 during the cell cycle has not yet been clearly documented, the observed fluctuations in p19 and p18 expression conform to the predicted pattern, with both being induced as cells exit G$_1$. Moreover, although the enforced overexpression of p18 can arrest G$_1$ progression in cells expressing wild-type pRb, it is without effect in pRb-negative cells (17). The latter observations raise the possibility that all INK4 members might be subject to pRb regulation and may in turn be unable to induce cell cycle arrest in pRb-negative cells. It will therefore be of interest to determine whether p19 and p18 also act as tumor suppressors.

ACKNOWLEDGMENTS

REFERENCES

1. **Anderson, S. J., M. A. Gonda, C. W. Rettenmier, and C. J. Sherr.** 1984. Subcellular localization of glycoproteins encoded by the viral oncogene v-*fms*. J. Virol. **51:**730–741.

2. **Baldin, V., J. Lukas, M. J. Marcote, M. Pagano, and G. Draetta.** 1993. Cyclin D1 is a nuclear protein required for cell cycle progression in G1. Genes Dev. **7:**812–821.

3. **Bartel, P. L., C.-T. Chien, R. Sternglanz, and S. Fields.** 1993. Using the two hybrid system to detect protein-protein interactions, p. 153–179. *In* D. A. Hartley (ed.), Cellular interactions in development: a practical approach. Oxford University Press, Oxford.

4. **Bates, S., L. Bonetta, D. Macallan, D. Parry, A. Holder, C. Dickson, and G. Peters.** 1994. CDK6 (PLSTIRE) and CDK4 (PSK-J3) are a distinct subset of the cyclin-dependent kinases that associate with cyclin D1. Oncogene **9:**71–79.

5. **Bates, S., D. Parry, L. Bonetta, K. Vousden, C. Dickson, and G. Peters.** 1994. Absence of cyclin D/cdk4 complexes in cells lacking functional retinoblastoma protein. Oncogene **9:**1633–1640.

6. **Caldas, C., S. A. Hahn, L. T. da Costa, M. S. Redston, M. Schutte, A. B. Seymour, C. L. Weinstein, R. H. Hruban, C. J. Yeo, and S. E. Kern.** 1994. Frequent somatic mutations and homozygous deletions of the p16 (MTS1) gene in pancreatic adenocarcinoma. Nature Genet. **8:**27–32.

7. **Chan, F. K. M., J. Zhang, L. Chen, D. N. Shapiro, and A. Winoto.** 1995. Identification of human and mouse p19, a novel CDK4 and CDK6 inhibitor with homology to p16^{ink4}. Mol. Cell. Biol. **15:**2682–2688.

8. **Chen, C., and H. Okayama.** 1987. High-efficiency transformation of mammalian cells by plasmid DNA. Mol. Cell. Biol. **7:**2745–2752.

9. **Dean, M., J. L. Cleveland, U. R. Rapp, and J. N. Ihle.** 1987. Role of *myc* in the abrogation of IL-3-dependence of myeloid FDC-P1 cells. Oncogene Res. **1:**279–296.

10. **Dowdy, S. F., P. W. Hinds, K. Louis, S. I. Reed, A. Arnold, and R. A. Weinberg.** 1993. Physical interactions of the retinoblastoma protein with human cyclins. Cell **73:**499–511.

11. **Downing, J. R., C. W. Rettenmier, and C. J. Sherr.** 1988. Ligand-induced tyrosine kinase activity of the colony-stimulating factor 1 receptor in a murine macrophage cell line. Mol. Cell. Biol. **8:**1795–1799.

12. **Downing, J. R., S. A. Shurtleff, and C. J. Sherr.** 1991. Peptide antisera to human colony-stimulating factor 1 receptor detect ligand-induced conformational changes and a binding site for phosphatidylinositol 3-kinase. Mol. Cell. Biol. **11:**2489–2495.

13. **Durfee, T., K. Becherer, P.-L. Chen, S.-H. Yeh, Y. Yang, A. Kilburn, W.-H. Lee, and S. J. Elledge.** 1993. The retinoblastoma protein associates with the protein phosphatase type 1 catalytic subunit. Genes Dev. **7:**555–569.

14. **El-Deiry, W. S., T. Tokino, V. E. Velculescu, D. B. Levy, R. Parsons, J. M. Trent, D. Lin, E. Mercer, K. W. Kinzler, and B. Vogelstein.** 1993. WAF1, a potential mediator of p53 tumor suppression. Cell **75:**817–825.

15. **Ewen, M. E., H. K. Sluss, C. J. Sherr, H. Matsushime, J. Kato, and D. M. Livingston.** 1993. Functional interactions of the retinoblastoma protein with mammalian D-type cyclins. Cell **73:**487–497.

16. **Gu, Y., C. W. Turek, and D. O. Morgan.** 1993. Inhibition of CDK2 activity *in vivo* by an associated 20K regulatory subunit. Nature (London) **366:**707–710.

17. **Guan, K., C. W. Jenkins, Y. Li, M. A. Nichols, X. Wu, C. L. O'Keefe, A. G. Matera, and Y. Xiong.** 1994. Growth suppression by p18, a p16$^{INK4/MTS1}$- and p14$^{INK4/MTS2}$-related CDK6 inhibitor, correlates with wild-type pRb function. Genes Dev. **8:**2939–2952.

18. **Hannon, G. J., and D. Beach.** 1994. p15^{INK4b} is a potential effector of cell cycle arrest mediated by TGF-β. Nature (London) **371:**257–261.

19. **Harper, J. W., G. R. Adami, N. Wei, K. Keyomarsi, and S. J. Elledge.** 1993. The p21 cdk-interacting protein Cip1 is a potent inhibitor of G1 cyclin-dependent kinases. Cell **75:**805–816.

20. **Hebert, J., J. M. Cayuela, J. Berkeley, and F. Sigaux.** 1994. Candidate tumor suppressor MTS1 (p16^{INK4A}) and MTS2 (p15^{INK4B}) display frequent homozygous deletions in primary cells from T- but not B-cell lineage acute lymphoblastic leukemias. Blood **84:**4038–4044.

21. **Hussussian, C. J., J. P. Struewing, A. M. Goldstein, P. A. T. Higgans, D. S. Ally, M. D. Sheahan, W. H. Clark, M. A. Tucker, and N. C. Dracopoli.** 1994. Germline p16 mutations in familial melanoma. Nature Genet. **8:**15–21.

22. **Kamb, A., N. A. Gruis, J. Weaver-Feldhaus, Q. Liu, K. Harshman, S. V. Tavtigian, E. Stockert, R. S. Day III, B. E. Johnson, and M. H. Skolnick.** 1994. A cell cycle regulator involved in genesis of many tumor types. Science **264:**436–440.

23. **Kamb, A., D. Shattuck-Eidens, R. Eeles, Q. Liu, N. A. Gruis, W. Ding, C. Hussey, T. Tran, Y. Miki, J. Weaver-Feldhaus, M. McClure, J. F. Aitken, D. E. Anderson, W. Bergman, R. Frants, D. E. Goldgar, A. Green, R. MacLennan, N. G. Martin, L. J. Meyer, P. Youl, J. J. Zone, M. H. Skolnick, and L. A. Cannon-Albright.** 1994. Analysis of the p16 gene (CDKN2) as a candidate for the chromosome 9p melanoma susceptibility locus. Nature Genet. **8:**22–26.

24. **Kato, J., H. Matsushime, S. W. Hiebert, M. E. Ewen, and C. J. Sherr.** 1993. Direct binding of cyclin D to the retinoblastoma gene product (pRb) and pRb phosphorylation by the cyclin D-dependent kinase, CDK4. Genes Dev. **7:**331–342.

25. **Look, A. T., S. L. Melvin, L. K. Brown, M. E. Dockter, P. K. Roberson, and S. B. Murphy.** 1984. Quantitative variation of the common acute lymphoblastic leukemia antigen (gp100) on leukemic marrow blasts. J. Clin. Invest. **73:**1617–1628.

26. **Lukas, J., H. Muller, J. Bartkova, D. Spitkovsky, A. A. Kjerulff, P. Jansen-Durr, M. Strauss, and J. Bartek.** 1994. DNA tumor virus oncoproteins and retinoblastoma gene mutations share the ability to relieve the cell's requirement for cyclin D1 function in G1. J. Cell. Biol. **125:**625–638.

27. **Matsuoka, M., J.-Y. Kato, R. P. Fisher, D. O. Morgan, and C. J. Sherr.** 1994. Activation of cyclin-dependent kinase-4 (cdk4) by mouse MO15-associated kinase. Mol. Cell. Biol. **14:**7265–7275.

28. **Matsushime, H., M. E. Ewen, D. K. Strom, J. Kato, S. K. Hanks, M. F. Roussel, and C. J. Sherr.** 1992. Identification and properties of an atypical catalytic subunit (p34^{PSKJ3}/CDK4) for mammalian D-type G1 cyclins. Cell **71:**323–334.

29. **Matsushime, H., D. E. Quelle, S. A. Shurtleff, M. Shibuya, C. J. Sherr, and J.-Y. Kato.** 1994. D-type cyclin-dependent kinase activity in mammalian cells. Mol. Cell. Biol. **14:**2066–2076.

30. **Matsushime, H., M. F. Roussel, R. A. Ashmun, and C. J. Sherr.** 1991. Colony-stimulating factor 1 regulates novel cyclins during the G1 phase of the cell cycle. Cell **65:**701–713.

31. **Meyerson, M., G. H. Enders, C. Wu, L. Su, C. Gorka, C. Nelson, E. Harlow, and L. Tsai.** 1992. The human cdc2 kinase family. EMBO J. **11:**2909–2917.

32. **Meyerson, M., and E. Harlow.** 1994. Identification of G$_1$ kinase activity for cdk6, a novel cyclin D partner. Mol. Cell. Biol. **14:**2077–2086.

33. **Mori, T., K. Miura, T. Aoki, T. Nishihira, N. Shozo, and Y. Nakamura.** 1994. Frequent somatic mutation of the MTS1/CDK4I (multiple tumor suppressor/cyclin-dependent kinase 4 inhibitor) gene in esophageal squamous cell carcinoma. Cancer Res. **54:**3396–3397.

34. **Muller, A. J., J. C. Young, A.-M. Pendergast, M. Pondel, N. R. Landau, D. R. Littman, and O. N. Witte.** 1994. *BCR* first exon sequences specifically activate the *BCR/ABL* tyrosine kinase oncogene of Philadelphia chromosome-positive human leukemias. Mol. Cell. Biol. **11:**1785–1792.

35. **Nobori, T., K. Miura, D. J. Wu, A. Lois, K. Takabayashi, and D. A. Carson.** 1994. Deletions of the cyclin-dependent kinase-4 inhibitor gene in multiple human cancers. Nature (London) **368:**753–756.

36. **Ogawa, S., N. Hirano, N. Sato, T. Takahashi, A. Hangaishi, K. Tanaka, M. Kurokawa, T. Tanaka, K. Mitani, Y. Yazaki, and H. Hirai.** 1994. Homozygous loss of the cyclin-dependent kinase-4 inhibitor (p16) gene in human leukemias. Blood **84:**2431–2435.

37. **Okamoto, A., D. J. Demetrick, E. A. Spillare, K. Hagiwara, S. P. Hussain, W. P. Bennett, K. Forrester, B. Gerwin, M. Serrano, D. H. Beach, and C. C. Harris.** 1994. Mutations and altered expression of p16^{INK4} in human cancer. Proc. Natl. Acad. Sci. USA **91:**11045–11049.

38. **Okuda, T., H. Hirai, J. D. Downing, V. Valentine, and C. J. Sherr.** 1995. Unpublished data.

39. **Otterson, G. A., R. A. Kratzke, A. Coxon, Y. W. Kim, and F. J. Kaye.** 1994. Absence of p16^{INK4} protein is restricted to the subset of lung cancer lines that retains wildtype RB. Oncogene **9:**3375–3378.

40. **Pear, W., G. Nolan, L. Martin, and D. Baltimore.** 1993. Production of higher-titer helper-free retroviruses by transient transfection. Proc. Natl.

41. **Pines, J., and T. Hunter.** 1990. Human cyclin A is adenovirus E1A-associated protein p60 and behaves differently from cyclin B. Nature (London) **346:**760–763.

42. **Polyak, K., J. Kato, M. J. Solomon, C. J. Sherr, J. Massague, J. M. Roberts, and A. Koff.** 1994. p27^{Kip1}, a cyclin-cdk inhibitor, links transforming growth factor-β and contact inhibition to cell cycle arrest. Genes Dev. **8:**9–22.

43. **Polyak, K., M. Lee, H. Erdjument-Bromage, A. Koff, J. M. Roberts, P. Tempst, and J. Massagué.** 1994. Cloning of p27^{Kip1}, a cyclin-dependent kinase inhibitor and a potential mediator of extracellular antimitogenic signals. Cell **78:**59–66.

44. **Quelle, D. E., R. A. Ashmun, S. A. Shurtleff, J. Kato, D. Bar-Sagi, M. F. Roussel, and C. J. Sherr.** 1993. Overexpression of mouse D-type cyclins accelerates G$_1$ phase in rodent fibroblasts. Genes Dev. **7:**1559–1571.

45. **Serrano, M., G. J. Hannon, and D. Beach.** 1993. A new regulatory motif in cell cycle control causing specific inhibition of cyclin D/cdk4. Nature (London) **366:**704–707.

46. **Sherr, C. J.** 1993. Mammalian G$_1$ cyclins. Cell **73:**1059–1065.

47. **Spruck, C. H., M. Gonzalez-Zulueta, A. Shibata, A. R. Simoneau, M.-F. Lin, F. Gonzales, Y. C. Tsai, and P. A. Jones.** 1994. p16 gene in uncultured tumors. Nature (London) **370:**183–184.

48. **Stanley, E. R.** 1986. The macrophage colony stimulating factor, CSF-1. Methods Enzymol. **116:**564–587.

49. **Tam, S. W., A. M. Theodoras, J. W. Shay, G. F. Draetta, and M. Pagano.** 1994. Differential expression and regulation of cyclin D1 protein in normal and tumor human cells: association with cdk4 is required for cyclin D1 function in G1 progression. Oncogene **9:**2663–2674.

50. **Toyoshima, H., and T. Hunter.** 1994. p27, a novel inhibitor of G1 cyclin/cdk protein kinase activity, is related to p21. Cell **78:**67–74.

51. **Tushinski, R. J., and E. R. Stanley.** 1985. The regulation of mononuclear phagocyte entry into S phase by the colony stimulating factor CSF-1. J. Cell. Physiol. **122:**221–228.

52. **Xiong, Y., G. J. Hannon, H. Zhang, D. Casso, R. Kobayashi, and D. Beach.** 1993. p21 is a universal inhibitor of cyclin kinases. Nature (London) **366:**701–704.

53. **Xiong, Y., H. Zhang, and D. Beach.** 1992. D-type cyclins associate with multiple protein kinases and the DNA replication and repair factor PCNA. Cell **71:**505–514.

54. **Xiong, Y., H. Zhang, and D. Beach.** 1993. Subunit rearrangement of the cyclin-dependent kinases is associated with cellular transformation. Genes Dev. **7:**1572–1583.

55. **Zamoyska, R., A. C. Vollmer, K. C. Sizer, C. W. Liaw, and J. R. Parnes.** 1985. Two lyt-2 polypeptides arise from a single gene by alternative splicing patterns of mRNA. Cell **43:**153–163.

56. **Zhang, H., G. J. Hannon, and D. Beach.** 1994. p21-containing cyclin kinases exist in both active and inactive states. Genes Dev. **8:**1750–1758.

Acad. Sci. USA **90:**8392–8396.